Enhancement of the cytotoxic potential of the mixed EGFR and DNA-targeting 'combi-molecule' ZRBA1 against human solid tumour cells by a bis-quinazoline-based drug design approach

Sherin Al-Safadi[a], Juozas Domarkas[b], YingShan Han[a], Fouad Brahimi[a] and Bertrand J. Jean-Claude[a]

ZRBA1 is a quinazoline-based molecule termed 'combi-molecule' designed to block the epidermal growth factor receptor (EGFR) and further degrade to FD105, an EGFR inhibitor plus a DNA-alkylating agent. To augment the potency of ZRBA1, we designed JDE52, a bistriazene that, following degradation, was 'programmed' to yield higher concentrations of the free inhibitor FD105 and a more cytotoxic bifunctional DNA-damaging species. The results indicated that JDE52 was capable of inducing significant blockade of EGFR phosphorylation, DNA strand breaks and interstrand cross-links in human cells. The fluorescent property of FD105, the secondary inhibitor that both JDE52 and ZRBA1 are capable of releasing, has permitted the analysis of its levels in tumour cells by ultraviolet flow cytometry. It was found that JDE52 was indeed capable of significantly releasing higher levels of fluorescence ($P < 0.05$) in human tumour cells when compared with ZRBA1. Apoptosis was triggered by JDE52 at a faster rate than ZRBA1 and led to higher levels of cell killing. The results *in toto* suggest that the superior potency of JDE52, when compared with ZRBA1, may be imputed to mechanisms associated with the generation of higher intracellular concentrations of FD105 and to the induction of DNA cross-links. These combined mechanisms (blockade of EGFR-tyrosine kinase and induction of cross-links) contributed to an accelerated rate of apoptosis by JDE52. This study conclusively demonstrated that designing molecules as prodrugs of high levels of quinazoline inhibitors of EGFR and bifunctional DNA cross-linking species is a valid strategy to enhance the potency of mixed EGFR-DNA-targeting combi-molecules. *Anti-Cancer Drugs* 23:483–493 © 2012 Wolters Kluwer Health | Lippincott Williams & Wilkins.

Anti-Cancer Drugs 2012, **23**:483–493

Keywords: apoptosis, combi-molecule, DNA damage, epidermal growth factor receptor, quinazoline, triazene, tyrosine kinase

[a]Cancer Drug Research Laboratory, Department of Medicine, McGill University Health Center/Royal Victoria Hospital, Division of Medical Oncology, Montreal, Quebec, Canada and [b]John Mallard Scottish P.E.T. Centre, School of Medical Sciences, University of Aberdeen, Foresterhill, UK

Correspondence to Bertrand J. Jean-Claude, PhD, Royal Victoria Hospital/McGill University Health Center, 687 Pine Avenue West Rm M-719, Montreal, Quebec, Canada H3A 1A1
Tel: +1 514 843 1231x35841; fax: +1 514 843 1475;
e-mail: bertrandj.jean-claude@mcgill.ca

Received 6 September 2011 **Revised form accepted** 24 January 2012

Introduction

Throughout the past decade, a paradigm shift has occurred in the field of drug development, moving from traditional receptor-specific drugs to a more recent cross-receptor view [1–4]. The current trend leans towards the development of drugs that are able to target not only one but multiple members of a receptor family [5–7]. Recently, we took this multitargeted approach a step further by designing not only drugs to target a receptor but also different macromolecules involved in the proliferation of cancer cells. The first examples designed were based on the class of drugs termed 'triazenes' [8–11]. These molecules, termed combi-molecules, clearly demonstrated the ability to block epidermal growth factor receptor-tyrosine kinase (EGFR-TK) and simultaneously damage DNA [12–14]. As one such example, SMA41 was shown to be more potent than a combination of temozolomide (a DNA-damaging agent) and SMA52 (an inhibitor of EGFR) [15]. Our fundamental premise for the development of such molecules was that downregulation of receptor-dependent signalling could lead to a depletion of the levels of DNA repair enzymes required to reverse lesions induced by the DNA-damaging property of the combi-molecule [16–19]. Recently, we developed ZRBA1 (Scheme 1), a molecule that showed significant activity *in vivo* in an MDA-MB-468 human breast tumour model [14]. However, its in-vitro inhibitory concentration (IC_{50}) for growth inhibition was in the high 20 μmol/l range in many tumour cells [14,20]. To enhance the potency of this type of molecules, we redesigned them to induce aggressive cross-linking lesions and degrade to a higher titre of inhibitors. Here, we describe the potency and mechanism of action of one such molecule designated as JDE52. ZRBA1 contains a dimethylethylamino moiety, which, after degradation, is converted to the short-lived dimethylethyl diazonium, leading to the formation of a mono-alkylating agent [14].

0959-4973 © 2012 Wolters Kluwer Health | Lippincott Williams & Wilkins DOI: 10.1097/CAD.0b013e328351c101

In contrast, JDE52 is an extension of ZRBA1, wherein one methyl group is replaced by an additional ethyltriazenoquinazoline moiety, leading to a system that when hydrolysed (see Scheme 2) will produce a nitrogen mustard-like species methyldiazonium (TZ), plus perhaps two moles of the aminoquinazoline FD105 (I), a molecule that is known to strongly inhibit EGFR (Scheme 2). FD105 fluoresces in the blue (451 nm), upon excitation at 290 nm. This unique property has permitted the analysis of its release in the intracellular compartment by fluorescence microscopy. The main purpose of this study was primarily to determine whether the newly designed

Scheme 1

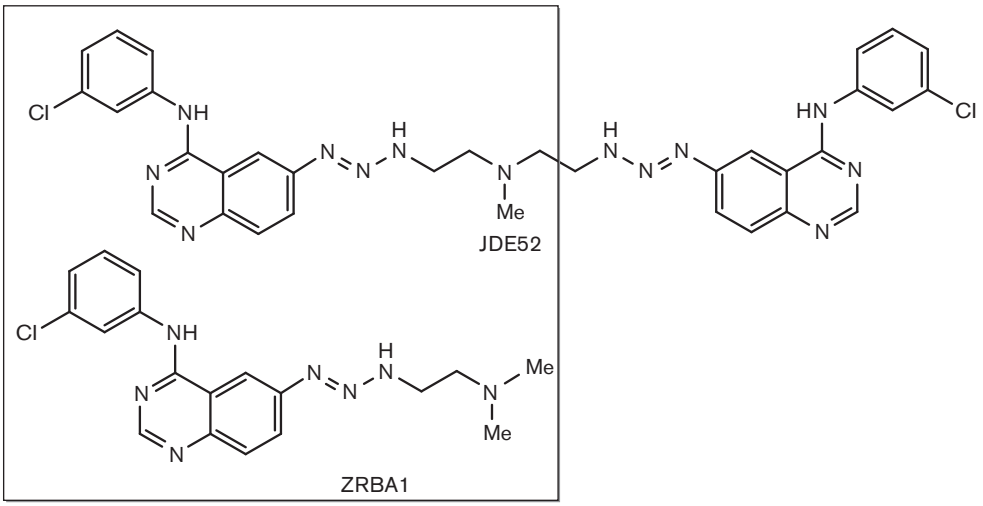

ZRBA1, a quinazoline-based combi-molecule, and JDE52, the bistriazene counterpart redesigned to augment the potency of ZRBA1.

Scheme 2

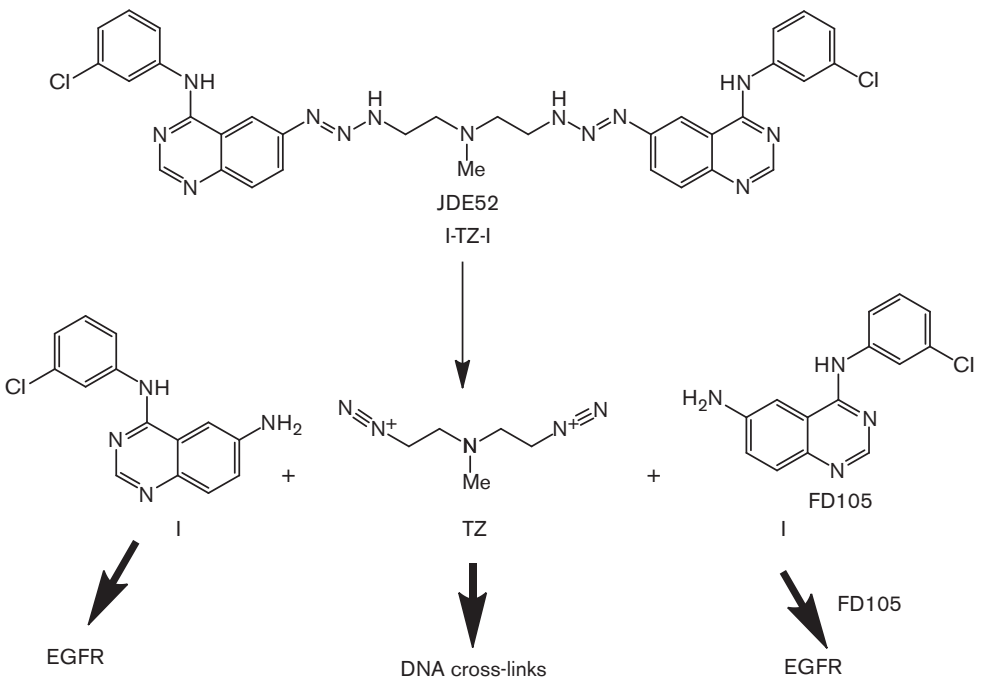

When hydrolysed, JDE52 produces a nitrogen mustard-like species methyldiazonium (TZ), plus perhaps 2 moles of the aminoquinazoline FD105 (I), an inhibitor of EGFR. EGFR, epidermal growth factor receptor.

combi-molecule would release higher levels of FD105, induce stronger blockade of EGFR phosphorylation and more cytotoxic DNA damage than ZRBA1, thereby triggering higher levels of apoptosis and cell killing than the latter drug in human tumour cells [21–25].

Methods

Drug treatment

ZRBA1 and JDE52 were synthesized in our laboratories (Cancer Drug Research Laboratory, MUHC, McGill University, Montreal, Quebec, Canada). In all assays, the drug was dissolved in dimethyl sulfoxide (DMSO) and subsequently diluted in sterile Roswell Park Memorial Institute medium (RPMI-1640), containing 10% fetal bovine serum (FBS) (Wisent, St Bruno, Quebec, Canada) immediately before the treatment of cell cultures [concentration of DMSO never exceeded 0.2% (v/v)].

Cell culture

The cell lines used in this study were the human prostate cancer DU145 cell line, obtained from the American Type Culture Collection (Manassas, Virginia, USA), and the human isogenic breast carcinoma cell line MDA-MB-435 (stably transfected with the ErbB2 and EGFR genes), which were generous gifts from Dr Moulay Aloui-Jamali (Montreal Jewish General Hospital, Montreal, Canada). Transfection of MDA-MB-435 cells was performed according to methods described by Yen *et al.* [26]. Western blot analysis confirming the differential levels of EGFR and ErbB2 in these cells has already been reported by our group elsewhere [27,28]. All cell lines were maintained in RMPI-1640 medium supplemented with 10% FBS, and with antibiotics as described previously [14]. Cells were maintained in a monolayer at 37°C in a humidified environment of 5% CO_2, 95% air. The cultures were maintained in exponential growth by harvesting with a trypsin-EDTA solution containing 0.5 mg/ml trypsin and 0.2 mg/ml EDTA and replating before confluence. In all assays, the cells were plated for 24–48 h before drug administration.

Degradation

The study of the conversion of JDE52 to FD105 was performed by spectrofluorimetry as the latter amine was fluorescent (absorption 290 nm, emission 451 nm). A 50 mmol/l stock solution of JDE52 in DMSO was added to RPMI-1640 with 10% FBS and incubated overnight at 37°C in a microplate spectrofluorimeter. The data were analysed using the SoftMaxPro (Molecular Devices, LLC, Sunnyvale, California, USA) and Graphpad software packages (GraphPad Software, La Jolla, California, USA).

Fluorescence microscopy imaging for intracellular release of the amine

DU145 cells were seeded in RPMI with 10% FBS for 24 h and grown in six-well plates (1×10^6/well). Cells were then treated with varying concentrations of ZRBA1 or JDE52 for 2 h and the medium was replaced with drug-free medium in each well. Thereafter, the plates were analysed using a Zeiss LSM 510 confocal microscope (Carl Zeiss MicroImaging GmbH, Gottingen, Germany), and cells were excited at 451 nm; emission was at 340 nm.

Ultraviolet flow cytometric analysis of intracellular fluorescence

DU145, MDA-MB-435, MDA-MB-435/EGFR and MDA-MD-435/ErbB2 were seeded in RPMI or Dulbecco's Modified Eagle Medium with 10% FBS for 24 h and grown in six-well plates (1×10^6/well). Cells were then treated with varying concentrations of ZRBA1 or JDE52 and 10% FBS at 37°C for 2 h. Thereafter, cells were harvested with trypsin-EDTA, subsequently collected by centrifugation and resuspended in PBS. Fluorescence levels were measured using the BD LSR flow cytometer (Becton Dickinson, Oakville, Ontario, Canada).

Epidermal growth factor receptor kinase assay

The EGFR kinase assay was performed as described previously [10,14–16]. Briefly, MaxiSorp 96-well plates (Nalgen Nunc International, Naperville, Illinois, USA) were incubated overnight at 37°C with 100 ml/well of 0.25 ng/ml poly[L-glutamic acid–L-tyrosine, 4 : 1] (PGT) in PBS. Excess PGT was removed and the plates washed three times with washing buffer (0.1% Tween 20 in PBS). The kinase reaction was performed with 4.5 ng/well of EGFR. Drugs were added and phosphorylation initiated by the addition of ATP (50 µmol/l). After 8 min at room temperature with constant shaking, the reaction was terminated by aspiration of the reaction buffer and rinsing the plate four times with washing buffer. Phosphorylated poly(Glu:Tyr)4 : 1 (PGT) was detected after a 25 min incubation with 50 µl/well of horseradish peroxidase-conjugated PY20 antiphosphotyrosine antibody (Santa Cruz Biotechnology, Santa Cruz, California, USA) diluted to 0.2 mg/ml in blocking buffer (3% bovine serum albumin and 0.05% Tween 20 in PBS). The antibody was removed and the plate washed four times with washing buffer. The signals were developed by the addition of 50 µl/well 3,5,3′,5′-tetramethylbenzidine peroxidase substrate (Kirkegaard and Perry Laboratories, Gaithersburg, Maryland, USA). On appearance of a persistent blue colour, a solution of sulfuric acid (50 µl, 0.09 mol/l) was added per well to stop the reaction. The plates were read at 450 nm using a Bio-Rad ELISA reader (model 2550; Bio-Rad, Hercules, California, USA).

Epidermal growth factor receptor phosphorylation assay

DU145 cells (1×10^6) were preincubated in a six-well plate with 10% serum at 37°C for 24 h and starved overnight for 24 h, after which they were exposed to a dose range of each drug for 2 h. Thereafter, they were treated with 50 ng/ml EGF for 15 min at 37°C. Cells were washed with PBS and resuspended in cold lysis buffer [50 mmol/l Tris-HCl pH 7.5; 150 mmol/l NaCl; 1%

Nonidet P-40, 1 mmol/l EDTA; 5 mmol/l NaF; 1 mmol/l Na_3VO_4; protease inhibitor tablet (Roche Biochemicals, Laval, Canada)]. The lysates were kept on ice for 30 min and collected by centrifugation at 10 000 rpm for 20 min at 4°C. The concentrations of protein were determined using the Bio-Rad protein assay kit (Bio-Rad Laboratories). Equal amounts of protein were added to a 10% SDS-polyacrylamide gel electrophoresis and transferred to a polyvinylidene difluoride membrane (Millipore, Bedford, Massachusetts, USA). Nonspecific binding on the membranes was minimized with a blocking buffer containing nonfat dry milk (5%) in phosphate buffered saline with Tween 20. Thereafter, the membranes were incubated with primary antiphosphotyrosine antibody (Upstate Biotechnology, Lake Placid, New York, USA) for the detection of phosphotyrosine. Membranes were stripped and reprobed with anti-EGFR (Neomarkers, Fremont, California, USA) for detection of corresponding receptor levels. Blots were incubated with horseradish peroxidase-goat anti-mouse antibody (1 : 1000 dilution; Cell Signaling Research, Beverly, Massachusetts, USA) and the bands visualized with an enhanced chemiluminescence system (Amersham Pharmacia Biotech, Little Chalfont, UK).

Growth inhibition assay

For nonstimulated cell growth inhibition, approximately 10×10^3 cells/well were plated in 96-well plates. After 24 h incubation at 37°C, cell monolayers were exposed to different concentrations of each drug continuously for 72 h. All growth inhibitory activities were evaluated using the sulforhodamine B (SRB) assay. Briefly, following drug treatment, cells were fixed using 50 µl of cold trichloroacetic acid (50%) for 60 min at 4°C, washed four times with tap water and stained for 30 min at room temperature with SRB (0.4%) dissolved in acetic acid (0.5%). The plates were rinsed five times with 1% acetic acid and allowed to air dry. The resulting coloured residue was dissolved in 200 µl of Tris-base (10 mmol/l), and optical density was read for each well at 540 nm using a Bio-Rad microplate reader (model 2550). Each point represents the average of at least two independent experiments run in triplicate. IC_{50} values were calculated using the median effect equation [29].

Alkaline comet assay for quantification of single-strand breaks

The modified alkaline comet assay was performed as previously described [15]. For in-vitro analysis, 8×10^5 cells were exposed to a dose range of either drug (ZRBA1 and JDE52) for 24 h, harvested with trypsin-EDTA, washed with PBS and collected by centrifugation (1.6*g* for 5 min). The supernatant was collected and the cells washed three times with cold PBS. For comet analysis, cell suspensions were diluted to an approximated 1×10^6 cells and mixed with agarose (1%) at 37°C in a 1 : 10 dilution. The gels were cast on Gelbond strips (Mandel Scientific, Guelph, Ontario, Canada) using gel casting chambers, as previously described, and then immediately placed into lysis buffer [2.5 mol/l NaCl, 0.1 mol/l tetra-sodium EDTA, 10 mmol/l Tris-base, 1% (w/v) *N*-lauryl sarcosine, 10% (v/v) DMSO, and 1% (v/v) Triton X-100, pH 10.0]. After being kept overnight at 4°C, the gels were gently rinsed with distilled water and immersed in a second lysis buffer (2.5 mol/l NaCl, 0.1 mol/l tetra-sodium EDTA, 10 mmol/l Tris-base containing 1 mg/ml proteinase K) for 60 min at 37°C. Thereafter, they were rinsed with distilled water, incubated in alkaline electrophoresis buffer for 30 min at 37°C and electrophoresed at 300 mA for 20 min. The gels were subsequently rinsed with distilled water and placed in 1 mol/l ammonium acetate for 30 min. Thereafter, they were soaked in 100% ethanol for 2 h, dried overnight and stained with SYBR Gold (1 : 10 000 dilution of stock supplied from Molecular Probes, Eugene, Oregon, USA) for 30 min. Comets were visualized at × 330 magnification and DNA damage was quantified using the tail moment parameter (i.e. the distance between the barycentre of the head and the tail of the comet multiplied by the percentage of DNA within the tail of the comet). A minimum of 25 cell comets were analysed for each sample as previously described [30,31], using ALKOMET version 3.1 image analysis software (Richard Branker Research, Ottawa, Canada), and values represent calculated means of tail moments for the entire cell population.

Alkaline unwinding assay

DU145 cells were seeded in RPMI with 10% FBS for 24 h and grown in six-well plates (1×10^6/well). Cells were then treated with 5 and 10 µmol/l of ZRBA1 or JDE52 for 2 h and washed twice with PBS. Following scraping of the cells in PBS, 1×10^6 cells were harvested by centrifugation, and the pellet generated was resuspended in 1 ml PBS. DNA was extracted using the GenElute Mammalian Genomic DNA miniprep kit (supplied by Sigma Aldrich, St Louis, Missouri, USA). A 3 ml solution containing ethidium bromide (10 µg/ml), K_2HPO_4 (20 mmol/l) and EDTA (0.4 mmol/l), pH 12.1, was added to the extracted DNA for 30 min. The mixture was heated to 100°C for 5 min to denature the DNA and then cooled on ice for 6 min to allow the DNA to reanneal. Before the mixture was heated, the fluorescence was measured at a wave length of 525 nm, and after the mixture had cooled, the fluorescence was measured at a wave length of 580 nm. DNA cross-links were determined according to the following equation [32]:

$$C_t = \frac{(f_{after}/f_{before})_t - (f_{after}/f_{before})_u}{1-(f_{after}/f_{before})_u} \times 100\,\%,$$

where f_{before} and f_{after} are fluorescence intensities before and after heat denaturation for treated (t) and untreated (u) cells.

DAPI staining for apoptosis

DU145 prostate cancer cells were plated in six-well plates for 24 h, at which point they were observed as confluent.

The cells were treated with JDE52 or ZRBA1 for 24 h, washed twice with PBS and centrifuged. They were subsequently treated with 1 mg/ml 4′,6-diamidino-2-phenylindole (DAPI) (0.5 µl) for 5 min and washed twice again with PBS. Cells in PBS (5 µl) were mounted on a glass slide and observed by using a × 60 Zeiss LSM 510 confocal microscope lens.

Annexin V binding

Cells were grown in six-well plates until confluence and then incubated with the compounds for 48 h. The cells were then harvested, washed twice with PBS and centrifuged. Cells (10^5) were treated with annexin V–fluorescein isothiocyanate (FITC) and propidium iodide (PI) using the apoptosis detection kit (BD Bioscience Pharmingen, San Jose, California, USA) and the supplier's protocol. Annexin V-FITC and PI binding were analysed by flow cytometry. Data were collected using logarithmic amplification of both the FL1 (FITC) and FL2 (PI) channels. Quadrant analysis of coordinate dot plots was performed with CellQuest software (Becton Dickinson Biosciences, Mississauga, Ontario, Canada). Unstained cells were used to adjust the photomultiplier voltage and for compensation setting adjustment to eliminate spectral overlap between the FL1 and FL2 signals.

Results

Fluorescence analysis

We first demonstrated that JDE52 could decompose into a fluorescent species by monitoring its degradation under physiological conditions (Fig. 1a). Its half-life was determined by calculations based on the rate of formation of FD105 and was found to be 1 h. It was less stable than ZRBA1 for which we previously reported a half-life of 1.8 h [14]. Having found that JDE52 was capable of decomposing into a fluorescent molecule, we further observed its intracellular degradation by fluorescent microscopy after a 2 and 24 h drug treatment. Although analyses were achievable after a 2 h drug treatment, 24 h later most cells treated with JDE52 were killed, thereby compromising microscopic observation at this time point. Having designed JDE52 to generate higher levels of FD105 than ZRBA1, we expected higher fluorescence intensities in DU145 cells treated with JDE52 than in those exposed to ZRBA1 (Fig. 1b). Indeed, at the higher doses (5, 10 and 50 µmol/l), a marked difference in fluorescence intensities was observed, with cells treated with JDE52 showing higher levels of fluorescence (Fig. 1c). Ocular inspection of single cells (Fig. 1d) showed that the fluorescence was concentrated in the perinuclear region of the cells, indicating that perhaps the compound is trapped in this area of the cell where it decomposes to release the fluorescent FD105.

Fluorescence microscopy being a qualitative analysis, we repeated this experiment using ultraviolet flow cytometry to quantify the levels of fluorescence generated by each drug in the DU145 cells. Cells treated with JDE52 showed

Fig. 1

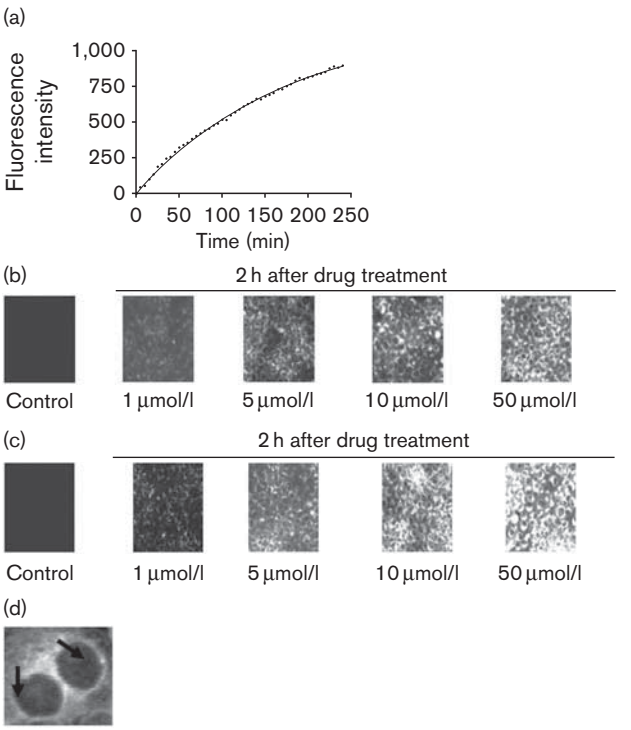

(a) Formation of free FD105 from JDE52. A solution of JDE52 was added to RPMI-1640 with 10% of FBS and incubated overnight at 37°C in a microplate spectrofluorimeter. The half-life of JDE52 was determined using first-order reaction kinetics based upon the rate of formation of FD105. Internalization of (b) ZRBA1 and (c) JDE52 in DU145 cells as revealed by fluorescence microscopy. Drugs were given for 2 h before observation. (d) Localization of FD105 around the perinuclear region of two DU145 cells treated with JDE52, as shown by confocal microsopy. FBS, fetal bovine serum; RPMI, Roswell Park Memorial Institute medium.

levels of fluorescence significantly higher ($P < 0.05$) at the high doses, when compared with ZRBA1 (Fig. 2a). To verify whether this type of distribution could be seen in other cell types, we analysed the intracellular degradation of ZRBA1 (Fig. 2b), JDE52 (Fig. 2c) and FD105 (Fig. 2d) in a panel of isogenic MDA-MB-435 breast cancer cells. We sought to verify whether the levels of EGFR or ErbB2 expressed in the cell could correlate with the levels of fluorescence intensities. We found that fluorescence emanated from JDE52 intracellular degradation was significantly higher in cells expressing EGFR than in the wild type. It is also to be noted that in these experiments, levels of FD105 generated by JDE52 were significantly higher compared with those generated by ZRBA1. Further, cells treated with pure FD105 alone showed significantly lower levels of intracellular fluorescence than those with JDE52, indicating that the latter behaved as a good prodrug of FD105 in the cells (Fig. 2d).

Growth inhibitory activity

The growth inhibitory effects of JDE52 were compared with those of ZRBA1 in the human DU145 prostate

Fig. 2

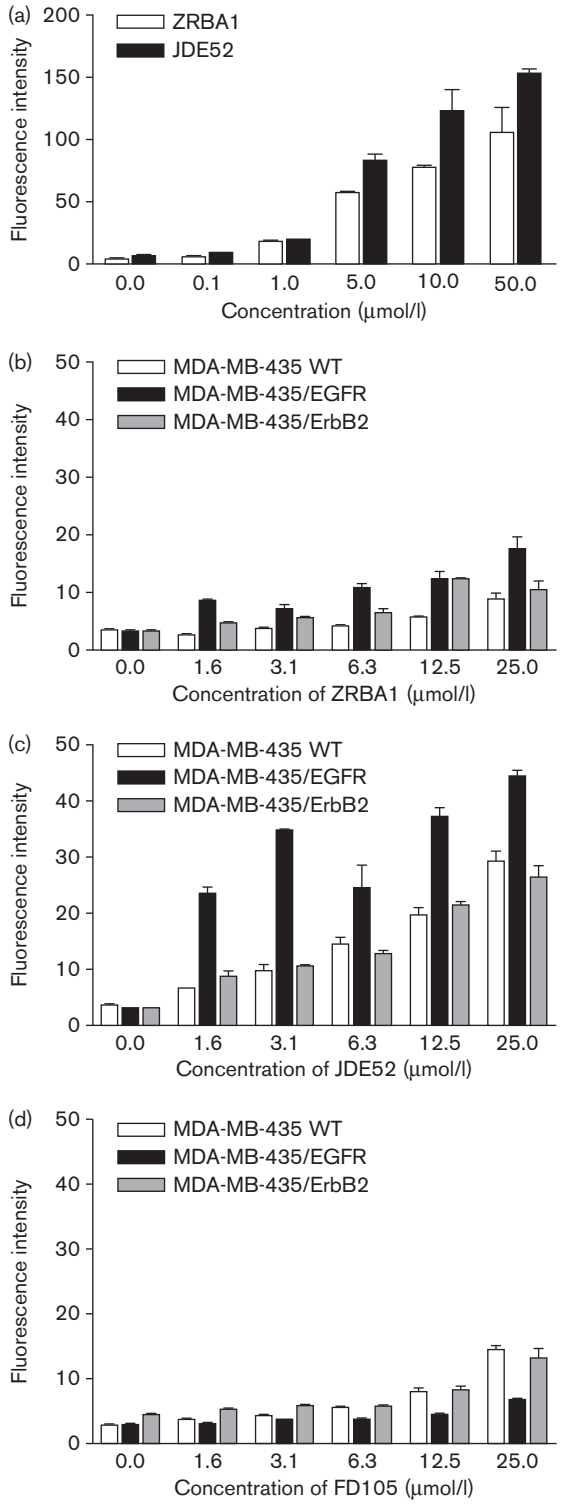

Ultraviolet flow cytometric analysis of intracellular levels of FD105 released by ZRBA1/JDE52 in DU145 cells (a), and in isogenic MDA-MB-435 cells (b, c), or FD105 alone treated isogenic MDA-MB-435 cells (d). Cells were treated with a dose range of ZRBA1 (b) or JDE52 (c) for 2 h before analysis. Each point represents at least two independent experiments run in duplicate. EGFR, epidermal growth factor receptor.

Fig. 3

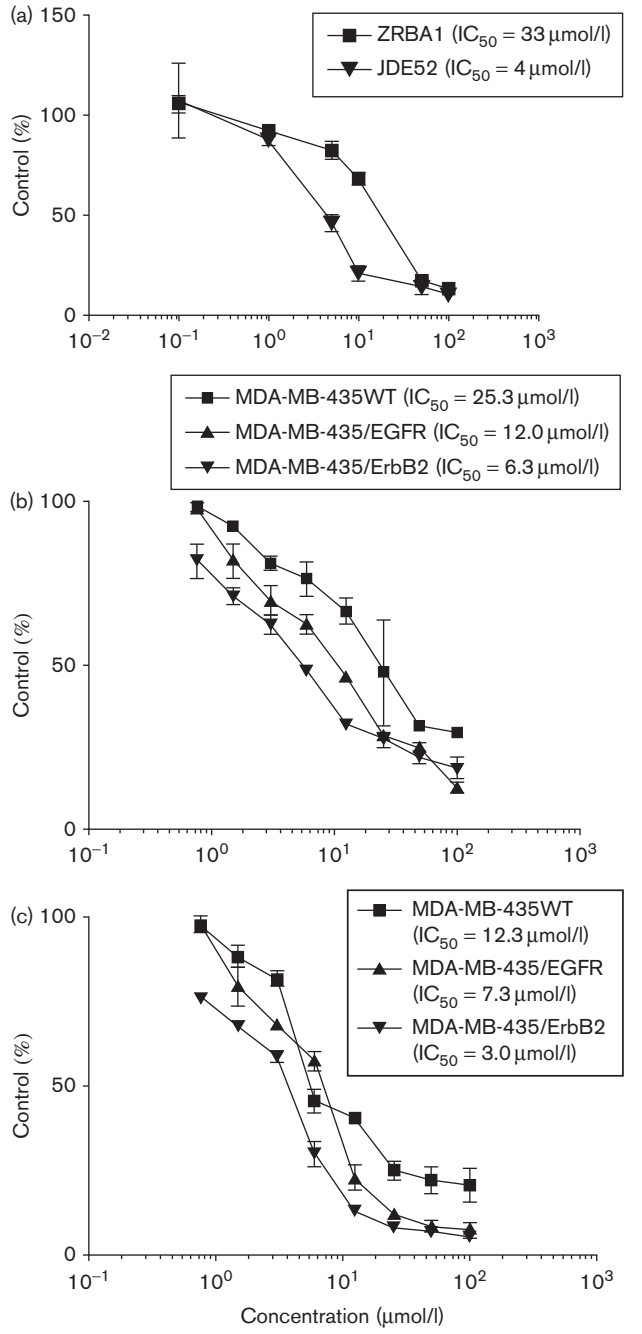

Effect of ZRBA1 and JDE52 on cell proliferation in DU145 cells (a), and in isogenic MDA-MB-435 cells (b, c). Cells were exposed to ZRBA1 or JDE52 for 72 h and growth inhibition was measured using the SRB assay. Each point represents at least two independent experiments run in triplicate. EGFR, epidermal growth factor receptor, IC_{50}, inhibitory concentration; SRB, sulforhodamine B.

cancer cell line and in the isogenic MDA-MB-435 cell line panel, using the SRB assay. The results showed that, in DU145 cells, JDE52 was eight-fold more potent than ZRBA1 (Fig. 3a). In the MDA-MB-435 isogenic cells, JDE52 was on average two-fold more potent than ZRBA1.

Fig. 4

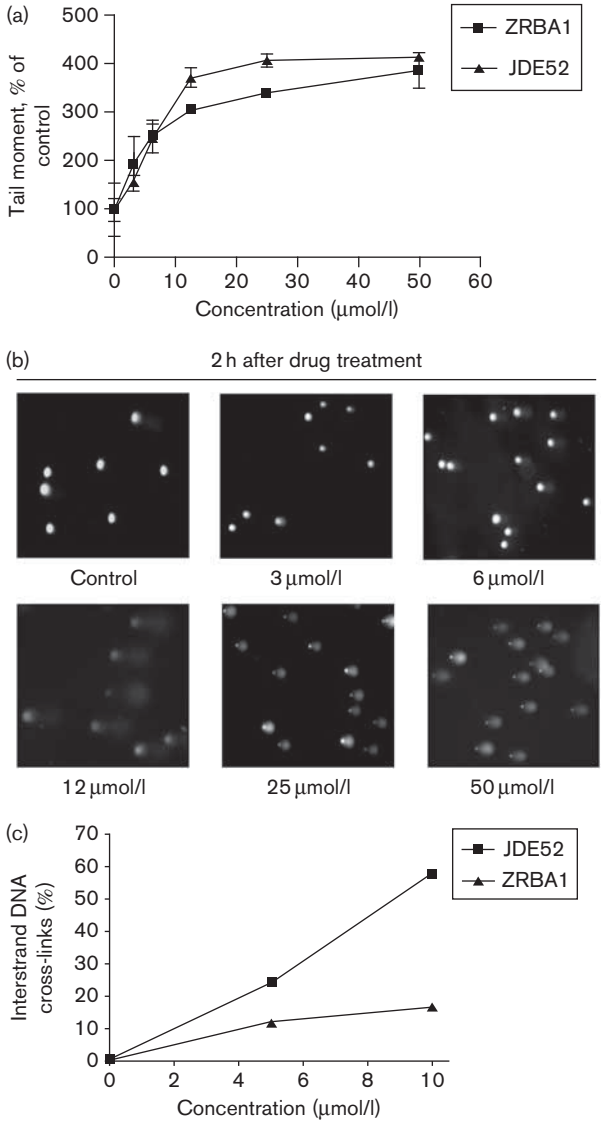

(a) Quantification of DNA damage using the alkaline comet assay. DNA damage induced by JDE52 or ZRBA1 in DU145 cell lines. Tail moment was used as a parameter for the detection of DNA damage in DU145 cells exposed to JDE52 or ZRBA1 for 2 h. Each point represents two independent experiments run in duplicate. (b) Representative images of DNA comets stained with SYBR Gold dye and visualized by fluorescence microscopy at $\times 330$ at different doses of JDE52. (c) JDE52 induces cross-link formation in DU145 prostate cells. DU145 cells were treated with a dose range of ZRBA1 or JDE52 for 2 h before analysis by a cross-linking assay.

Fig. 5

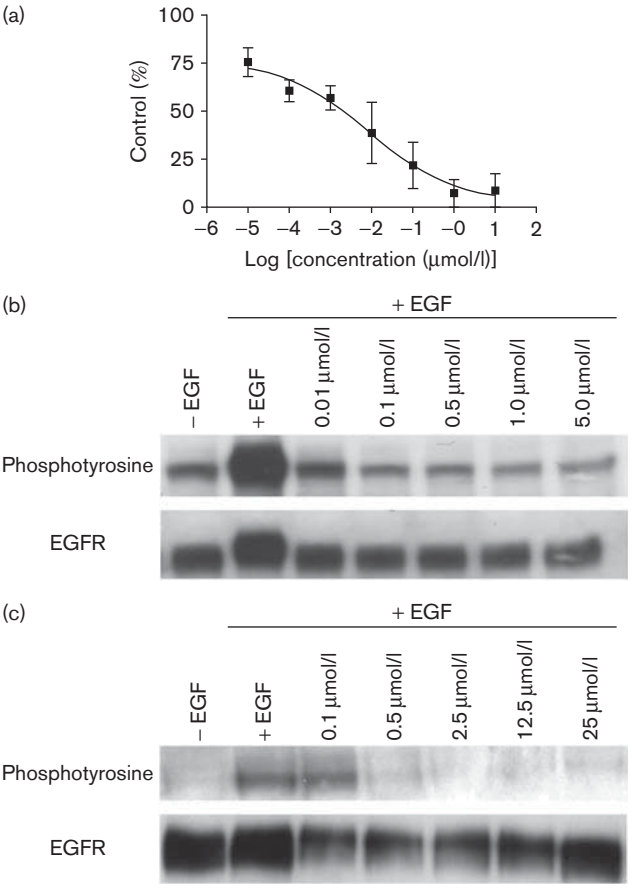

(a) Competitive binding to epidermal growth factor receptor by JDE52. Poly[L-glutamic acid–L-tyrosine, 4 : 1] substrate phosphorylation was detected using antiphosphotyrosine antibodies, after an 8-min drug exposure to the isolated EGFR-tyrosine kinase. Each point represents the average of two experiments run in duplicate. (b) Selective inhibition of EGFR autophosphorylation in DU145 cells by JDE52. Serum starved DU145 cells were preincubated for 2 h with the indicated concentrations of JDE52 before stimulation with EGF for 15 min. Equal amounts of cell lysates were analysed by western blotting using antiphosphotyrosine antibodies. Membranes were stripped of antiphosphotyrosine and reprobed with anti-EGFR antibodies as a loading control. (c) Selective inhibition of EGFR autophosphorylation in DU145 cells by ZRBA1. EGFR, epidermal growth factor receptor.

Interestingly, both compounds were more selective for the ErbB2 transfectants than the EGFR ones, with fold selectivity of around 1.6 for EGFR and 4 for ErbB2 (Fig. 3b and c).

DNA lesions induced by JDE52 in DU145 cells

As mentioned earlier, ZRBA1 is designed to degrade to a mono-alkylating agent, whereas JDE52 is supposed to generate a bifunctional cross-linking metastable species. Thus, we designed two sets of experiments, one to determine whether JDE52 could generate any type of damage and the other to determine levels of DNA cross-links. Total levels of DNA single-strand breaks were determined by micro-gel electrophoresis comet assay and DNA cross-linking by alkaline unwinding. The results showed that, similar to ZRBA1, JDE52 was capable of inducing dose-dependent DNA damage (Fig. 4a–b). Alkaline unwinding also showed that, in contrast to ZRBA1, JDE52 was capable of inducing significant levels of DNA cross-links (Fig. 4c).

Inhibition of epidermal growth factor phosphorylation by ZRBA1 and JDE52 in DU145 cells

In an isolated enzyme assay (Fig. 5a), JDE52 inhibited EGFR phosphorylation in a dose-dependent manner with an IC_{50} of 7.8 nmol/l. As shown in Fig. 5b, this inhibition translated into a dose-dependent blockade of EGF-induced EGFR phosphorylation in the human DU145 prostate cancer cells, with almost 100% inhibition at a concentration as low as 0.1 μmol/l. In contrast, at the same concentration, EGFR phosphorylation activity was not fully inhibited by ZRBA1 (Fig. 5c). Cell exposure being longer than the half-life of the combi-molecule, this strong effect may result from both the intact molecule and its degradation products.

Apoptosis

The DU145 cells overexpress EGFR and it has been shown that in these cells activation of EGFR leads to the activation of the antiapoptotic pathway through Akt and Bcl-2-associated death promoter phosphorylation. Therefore, we surmise that the potent inhibition by JDE52 in this cell line should alleviate the antiapoptotic pathway, thereby leading to apoptosis. Indeed, when cells were exposed to ZRBA1 or JDE52, formation of apoptotic cells with condensed nuclei was detected using DAPI staining (Fig. 6). Quantification with the annexin V binding assay showed that JDE52 and ZRBA1 were capable of inducing apoptosis in a dose-dependent manner. JDE52 triggered apoptosis at a much lower concentration than did ZRBA1 (Fig. 7a). Analysis of the necrosis quadrant also showed that JDE52 could induce higher levels of necrosis than ZRBA1, indicating its superior cytotoxicity over ZRBA1 (Fig. 7b–d).

Discussion

The combi-targeting strategy developed in our laboratory seeks to design molecules termed combi-molecules with affinity to target TK receptors and also programmed to degrade into another inhibitor of the same TK [13,14,33,34]. As depicted in Scheme 2, molecules termed TZ-I are designed to generate an alkylating moiety TZ + , an inhibitor I. To enhance the potency of the combi-molecule, here we designed a novel system to generate 2 moles of inhibitor plus a bifunctional alkylating agent. We surmised that the generation of a high titre of the inhibitor plus a more aggressive alkylating function would give rise to a combi-molecule with increased potency when compared with its mono-alkylating counterpart. ZRBA1 was an adequate comparative molecule, as it possessed almost the exact same moiety as JDE52 (see Scheme 1). In principle, JDE52 was expected to be a two-fold stronger inhibitor of EGFR and a stronger DNA-damaging agent than ZRBA1. However, degradation studies showed that the molecule generated less than 2 moles of FD105. This could be explained by the formation of by-products during the degradation of JDE52 that lowered the yield of FD105. However, its decomposition led to the generation of a higher yield of FD105 than that of its mono-alkyltriazene counterpart ZRBA1. Furthermore, as outlined in Scheme 2, we demonstrated that, in contrast to ZRBA1, the chemical mechanism of degradation of JDE52 leads to the formation of a species responsible for its ability to induce DNA intrastrand cross-links. Thus, JDE52 is the first combi-molecule capable of generating high levels of FD105, in addition to inducing DNA strand breaks and DNA interstrand cross-links in tumour cells.

One of the most important aspects of the study was to verify whether the new strategy will increase EGFR inhibitory potency. Given the expected high titre of FD105, a strong EGFR inhibitory potency was predicted

Fig. 6

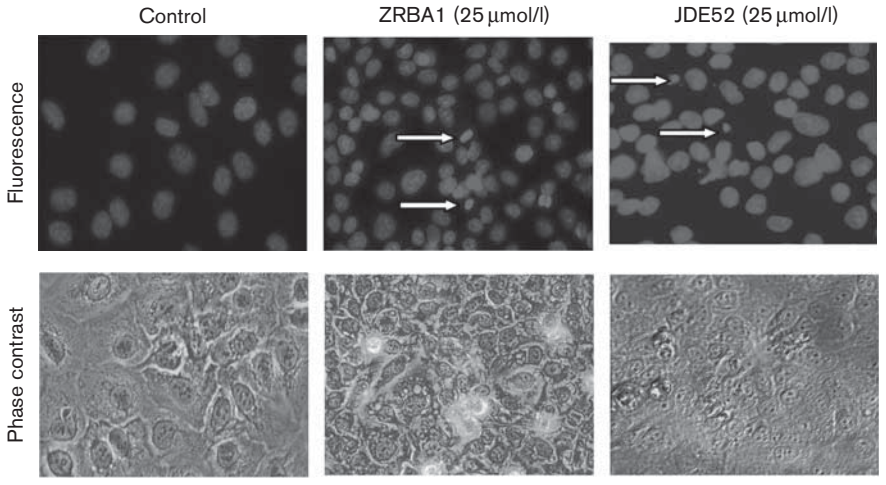

Drug-induced apoptosis in the DU145 prostate cancer cell line. Cells were treated with a dose range of ZRBA1 and JDE52 for 24 h and stained with DAPI, before observation of apoptotic cells by microscopy. DAPI, 4′,6-diamidino-2-phenylindole.

Fig. 7

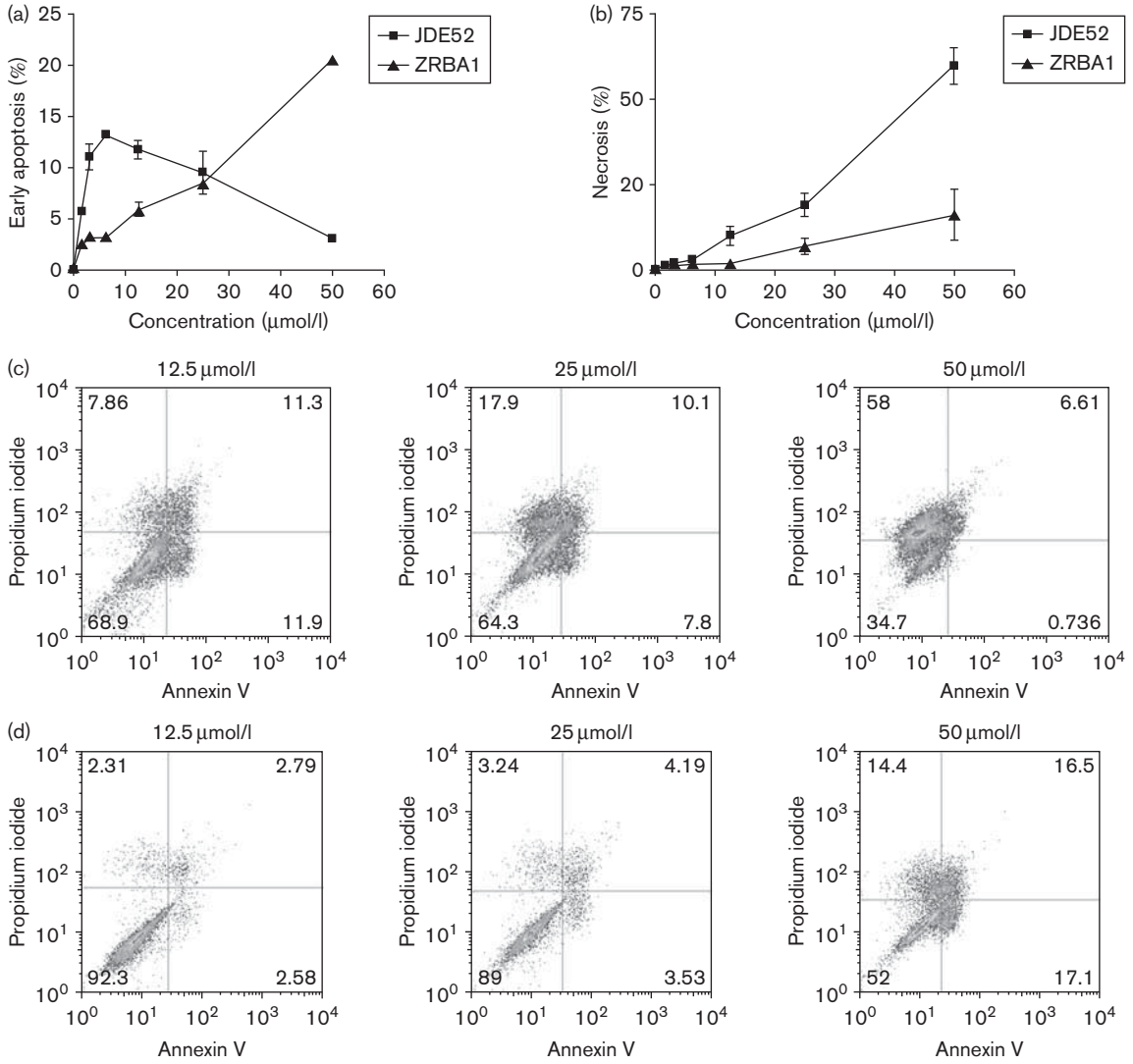

Assessment of: (a) apoptotic effects and (b) necrotic effects induced by ZRBA1 or JDE52. DU145 cells were treated with a dose range of ZRBA1 or JDE52 for 48 h. Levels of apoptotic cells were determined using annexin V-FITC staining. Each point represents two independent experiments run in duplicate. Representative dot plots obtained from annexin V/PI staining for quantifying apoptosis and necrosis induced by JDE52 (c) and ZRBA1 (d) in the DU145 cells. FITC, fluorescein isothiocyanate.

for this molecule. Indeed, the results showed that, at concentrations as low as 0.01 μmol/l, JDE52 was capable of significantly inhibiting EGFR phosphorylation in whole cells. The superior potency of JDE52 when compared with ZRBA1 was also translated in growth inhibitory assays. IC_{50} values of ZRBA1 were as previously reported in the 20 μmol/l range, whereas JDE52 values were as low as 3 μmol/l in tumour cells.

Although the potency of JDE52 was clearly evident in the cells, it was important to analyse the ability of this large molecule to block EGFR in isolated assays. As shown in Fig. 5a, JDE52, despite its bulkiness, was capable of strongly blocking EGFR-TK phosphorylation in a short 8-min exposure assay, a time point that was significantly shorter than the half-life of JDE52 under physiological conditions. The experiment was carried out at room temperature to prevent the degradation of the molecule. Indeed, molecular modelling in an independent study (J. Domarkas, Q. Qiyu, F. Brahimi, R. Banerjee, B.J. Jean-Claude, unpublished observation) has confirmed that one-half of the molecule could bind to the receptor, whereas the other half pointed away from the binding site, indicating that JDE52 is not only capable of degrading to another inhibitor in a high yield but is also able to bind to EGFR-TK as an intact structure.

Using the human prostate cancer DU145 cell line, which is known to undergo apoptosis upon blockade of EGFR, we confirmed that one of the mechanisms of cell death

induced by our molecule was apoptosis. The level of apoptosis induced by JDE52 was superior to that of ZRBA1, a result that may be explained by its high DNA-damaging potential and its strong EGFR inhibitory potency. Moreover, the subcellular distribution of JDE52 seems to have played a role in its potency. Indeed, it was found that significantly higher levels of fluorescence associated with FD105 was seen in cells transfected with EGFR, suggesting that the presence of the latter proteins in the cell may contribute to a retention of FD105. Although the direct involvement of the receptors in the abundance of FD105 is not clearly elucidated, it appears that the perinuclear region of the cell is the preferred localization of FD105. With the assumption that this correlates with the localization of intact JDE52, perhaps this preferential subcellular distribution also concentrated the release of the DNA-damaging species in the vicinity of the nucleus. It is also important to note that, despite the more abundant release of FD105 in EGFR-transfected cells when compared with its ErbB2 counterpart, both combi-molecules (JDE52 and ZRBA1) were more potent in the ErbB2 transfectants. This may perhaps be because of the fact that ErbB2 is playing a more proliferative role in the MDA-MB-435 transfectant than in its EGFR counterpart. However, further studies are required to elucidate this observation.

The study clearly demonstrates that a molecule with the size of JDE52 can be designed to not only bind to a receptor but also to degrade to multiple bioactive species directed at specific anticancer targets in the cell. This molecular programming seems to present the advantage of discrete subcellular distribution of the combi-molecule in the intracellular compartment. Although the significance of the perinuclear localization of FD105 in the cytotoxicity of JDE52 requires further studies, here we demonstrate that it can correlate with the levels of EGFR in the cell and with selective antiproliferative activity in human cancer cells. Thus, the molecule can be designed to enhance the potency of each targeted bioactive species [35,36]. This model may well represent a new avenue in the design of drugs capable of reversing the refractory mechanisms that protect advanced solid tumour cells against cytotoxic therapeutic agents [37].

Acknowledgements

This study was supported by grants from the Canadian Institutes of Health Research (CIHR).

Conflicts of interest

There are no conflicts of interest.

References

1 Lin S, Makino K, Xia W, Matin A, Wen Y, Kwong KY, *et al*. Nuclear localization of EGF receptor and its potential new role as a transcription factor. *Nat Cell Biol* 2001; **3**:802–808.
2 Lo H, Hsu S, Hung M. EGFR signaling pathway in breast cancers: from traditional signal transduction to direct nuclear translocalization. *Breast Cancer Res Treat* 2005; **95**:211–218.
3 Normanno N, De Luca A, Bianco C, Strizzi L, Mancino M, Maiello MR, *et al*. Epidermal growth factor receptor (EGFR) signaling in cancer. *Gene* 2006; **366**:2–16.
4 Pal S, Pegram M. Epidermal growth factor receptor and signal transduction: potential targets for anti-cancer therapy. *Anticancer Drugs* 2005; **16**: 483–494.
5 Zandi R, Larsen AB, Andersen P, Stockhausen MT, Poulsen HS. Mechanisms for oncogenic activation of the epidermal growth factor receptor. *Cell Signal* 2007; **19**:2013–2023.
6 Roskoski R Jr. The ErbB/HER receptor protein-tyrosine kinases and cancer. *Biochem Biophys Res Commun* 2004; **319**:1–11.
7 Burgess A, Cho H, Eigenbrot C, Ferguson K, Garrett T, Leahy D, *et al*. An open-and-shut case? Recent insights into the activation of EGF/ErbB receptors. *Mol Cell* 2003; **12**:541–552.
8 Rachid Z, Brahimi F, Katsoulas A, Teoh N, Jean-Claude BJ. The combi-targeting concept: chemical dissection of the dual targeting properties of a series of "combi-triazenes". *J Med Chem* 2003; **46**:4313–4321.
9 Qiu Q, Domarkas J, Banerjee R, Merayo N, Brahimi F, McNamee J, *et al*. The combi-targeting concept: in vitro and in vivo fragmentation of a stable combi-nitrosourea engineered to interact with the epidermal growth factor receptor while remaining DNA reactive. *Clin Cancer Res* 2007; **13**:331–340.
10 Qiu Q, Domarkas J, Banerjee R, Katsoulas A, McNamee J, Jean-Claude BJ. Type II combi-molecules: design and binary targeting properties of the novel triazolinium-containing molecules JDD36 and JDE05. *Anticancer Drugs* 2007; **18**:171–177.
11 Sabharwal A, Middleton M. Exploiting the role of O6-methylguanine-DNA-methyltransferase (MGMT) in cancer therapy. *Curr Opin Pharmacol* 2006; **6**:355–363.
12 Banerjee R, Rachid Z, McNamee J, Jean-Claude BJ. Synthesis of a prodrug designed to release multiple inhibitors of the epidermal growth factor receptor tyrosine kinase and an alkylating agent: a novel tumor targeting concept. *J Med Chem* 2003; **46**:5546–5551.
13 Brahimi F, Matheson S, Dudoit F, McNamee J, Tari A, Jean-Claude BJ. Inhibition of epidermal growth factor receptor-mediated signaling by "Combi-Triazene" BJ2000, a new probe for combi-targeting postulates. *J Pharm Exp Ther* 2002; **303**:832–840.
14 Brahimi F, Rachid Z, McNamee J, Alaoui-Jamali M, Tari A, Jean-Claude BJ. Mechanism of action of a novel "combi-triazene" engineered to possess a polar functional group on the alkylating moiety: evidence for enhancement of potency. *Biochem Pharmacol* 2005; **70**:511–519.
15 Matheson S, McNamee J, Wang T, Alaoui-Jamali M, Tari A, Jean-Claude BJ. The combi-targeting concept: dissection of the binary mechanism of action of the combi-triazene SMA41 in vitro and antitumor activity in vivo. *J Pharmacol Exp Ther* 2004; **311**:1163–1170.
16 Matheson S, Brahimi F, Jean-Claude BJ. The combi-targeting concept: intracellular fragmentation of the binary epidermal growth factor (EGFR)/DNA targeting "combi-triazene" SMA41. *Biochem Pharmacol* 2004; **67**:1131–1138.
17 Matheson S, McNamee J, Jean-Claude BJ. Design of a chimeric 3-methyl-1,2,3-triazene with mixed receptor tyrosine kinase and DNA damaging properties: a novel tumor targeting strategy. *J Pharmacol Exp Ther* 2001; **296**:832–840.
18 Matheson S, McNamee J, Jean-Claude BJ. Differential responses of EGFR-/AGT-expressing cells to the "combi-triazene" SMA41. *Cancer Chemother Pharmacol* 2003; **51**:11–20.
19 Middleton M, Margison G. Improvement of chemotherapy efficacy by inactivation of a DNA-repair pathway. *Lancet Oncol* 2003; **4**:37–44.
20 Heravi M, Rachid Z, Goudarzi A, Schlisser A, Jean-Claude BJ. Interaction of ionizing radiation and ZRBA1, a mixed EGFR/DNA-targeting molecule. *Anticancer Drugs* 2009; **20**:659–667.
21 Herr I, Debatin K. Cellular stress response and apoptosis in cancer therapy. *Blood* 2001; **98**:2603–2614.
22 Heymach J, Nilsson M, Blumenschein G, Papadimitrakopoulou V, Herbst R. Epidermal growth factor receptor inhibitors in development for the treatment of nonsmall cell lung cancer. *Clin Cancer Res* 2006; **12**:4441s–4445s.
23 Bogoyevitch M, Barr R, Ketterman A. Peptide inhibitors of protein kinases–discovery, characterization and use. *Biochim Biophys Acta* 2005; **1754**: 79–99.
24 Ying W, Sanders P. EGF receptor activity modulates apoptosis induced by inhibition of the proteasome of vascular smooth muscle cells. *J Am Soc Nephrol* 2007; **18**:131–142.
25 Zhang T, Xinmin C. Grb2 regulates Stat3 activation negatively in epidermal growth factor signalling. *Biochemical Society* 2003; **376**:457–464.
26 Yen L, Benlimame N, Nie ZR, Ziao D, Wang T, Al Moustafa AE, *et al*. Differential regulation of tumor angiogenesis by distinct ErbB homo- and heterodimers. *Mol Biol Cell* 2002; **13**:4029–4044.

27 Banerjee R, Huang Y, McNamee J, Todorova M, Jean-Claude BJ. The combi-targeting concept: selective targeting of the epidermal growth factor receptor- and Her2-expressing cancer cells by the complex combi-molecule RB24. *J Pharmacol Exp Ther* 2010; **334**:9–20.
28 MacPhee M, Rachid Z, Todorova M, Jean-Claude BJ. Characterization of the potency of the epidermal growth factor (EGFR)-DNA targeting combi-molecules containing a hydrolabile carbamate at the 3-position of the triazene chain. *Invest New Drugs* 2011; **20**:833–845.
29 Tchou T, Talalay P. Quantitative analysis of dose-effect relationships: the combined effects of multiple drugs or enzyme inhibitors. *Adv Enzyme Regul* 1984; **22**:27–55.
30 Olive P, Banath J. The comet assay: a method to measure DNA damage in individual cells. *Nat Protoc* 2006; **1**:23–29.
31 Joytchev G, Menke M, Schubert I. The comet assay detects adaptation to MNU-induced damage in barley. *Mutat Res* 2001; **493**:95–100.
32 Ueda-Kawamitsu H, Lawson T, Gwilt P. In vitro pharmacokinetics and pharmacodynamics of 1,3-bis(2-chloroethyl)-1-nitrosourea (BCNU). *Biochem Pharmacol* 2002; **63**:1209–1218.
33 Domarkas J, Qiyu Q, Brahimi F, Banerjee R, Jean-Claude BJ. The combi-targeting concept: synthesis of stable nitrosoureas designed to inhibit the epidermal growth factor receptor (EGFR). *J Med Chem* 2006; **49**:3544–3552.
34 Merayo N, Rachid Z, Qiu Q, Brahimi F, Jean-Claude BJ. The combi-targeting concept: evidence for the formation of a novel inhibitor in vivo. *Anticancer Drugs* 2006; **17**:165–171.
35 Zwick E, Ullrich A. Receptor tyrosine kinase signalling as a target for cancer intervention strategies. *Endocr Relat Cancer* 2001; **8**:161–173.
36 Wong R, Guillaud L. The role of epidermal growth factor and its receptors in mammalian CNS. *Cytokine Growth Factor Rev* 2004; **15**:147–156.
37 Hatake K, Tokudome N, Ito Y. Next generation molecular targeted agents for breast cancer: focus on EGFR and VEGFR pathways. *Breast Cancer Res Treat* 2007; **14**:132–149.